



Evaluation of Free Radical Quenching Ability of Quinoline Acids through *in vitro* and Theoretical Studies

S. KIRUTHIKA[✉] and V. SHARULATHA*[✉]

Department of Chemistry, Avinashilingam Institute for Home Science and Higher Education for Women, Coimbatore-641043, India

*Corresponding author: E-mail: sharulatha_chem@avinuty.ac.in

Received: 11 May 2023;

Accepted: 13 July 2023;

Published online: 31 July 2023;

AJC-21335

Drugs based antioxidants are commonly suggested as targets while designing new medicines. All sorts of pharmaceutical drug development benefit from the extremely desirable quinoline moiety with antioxidant. In this work, the scavenging behaviour of four quinoline derivatives (Q1-Q4) towards DPPH, H₂O₂, ABTS and superoxide activity were investigated. According to the *in vitro* inhibition concentration (IC₅₀), quinoline derivative Q1 showed high antioxidant potential. Additionally, the theoretical DFT gas phase calculations of HOMO-LUMO, MEP, NPA and NBO are used to study the conjugating systems in radicals and showed that the N-H site acts more favourable than the O-H site for the radical attack. The calculated bond dissociation energy (BDE) values demonstrated that compound Q1 follows the HAT mechanism and while the calculated ionization potential (IP) and proton dissociation energy (PDE) values showed that Q4 follows the SET-PT route. The results of these two mechanisms demonstrated that radical quenching activity occurs at the N-H and O-H sites. The spin density demonstrates that both radicals are delocalized uniformly across the molecule.

Keywords: Quinoline acids, Antioxidant, DPPH, ABTS, Hydrogen peroxide, Superoxide, Computational studies.

INTRODUCTION

The formation of free radicals is an unavoidable result of adenosine triphosphate (ATP) synthesis in the mitochondria of a cell. The free radicals generated include, reactive oxygen species (ROS) and reactive nitrogen species (RNS) [1]. These free radicals if not scavenged by antioxidants will interact with lipids, proteins and DNA to cause irreversible oxidative damage to the cells [2]. An antioxidant is a molecule that scavenges free radical and prevents oxidative damage of the tissues. In order to keep the human body in good condition, it is essential to strike a balance between the antioxidants and the free radicals. This oxidative stress for a prolonged period may lead to cancer, hypertension, diabetics, Parkinson's and Alzheimer's diseases [3-5]. Antioxidants help slow down the progression of Alzheimer's disease [6]. As a result, it is standard procedure in the pharmaceutical industry to generate therapeutic candidates to combat diseases like Alzheimer's and cancer.

Quinolines are the scaffolds that are immensely studied for their varied biological activity such as antimalarial [7], antitumour [8], antiviral [9], antifungal [10], antimicrobial [8], anti-inflammatory [10] and anticancer agents [7]. Numerous

studies have shown that quinolines, namely those with a 3,4-double bond and 2-oxo functionality in their structure, possess powerful radical scavenging characteristics [11-18].

Antioxidants may follow three fundamental mechanisms, which are hydrogen atom transfer (HAT), single electron transfer-proton transfer (SET-PT) and sequential proton loss electron transfer (SPLET) or coupled electron transfer. DFT calculations are most significant method for the analysis of mechanism of antioxidant molecules and also to assess the antioxidant potential of the molecules.

Given the relevance of the quinoline nucleus, the antioxidant properties of quinoline acids [19,20] such as [2-(4-methyl-2-oxo-1,2-dihydroquinolin-3-yl)acetic acid] (Q1), [2-(2-oxo-4-phenyl-1,2-dihydroquinoline-3-yl) acetic acid] (Q2), [3-(4-methyl-2-oxo-1,2-dihydroquinolin-3-yl)propanoic acid] (Q3) and [3-(2-oxo-4-phenyl-1,2-dihydroquinolin-3-yl)propanoic acid] (Q4) (Fig. 1) were investigated by *in vitro* and computational methods. These acids have two hydrogen abstraction sites, the N-H at 7th and O-H at 17th positions, respectively. Hence, these structural moieties can effectively scavenge radicals and thus can serve as a potent antioxidant agent.

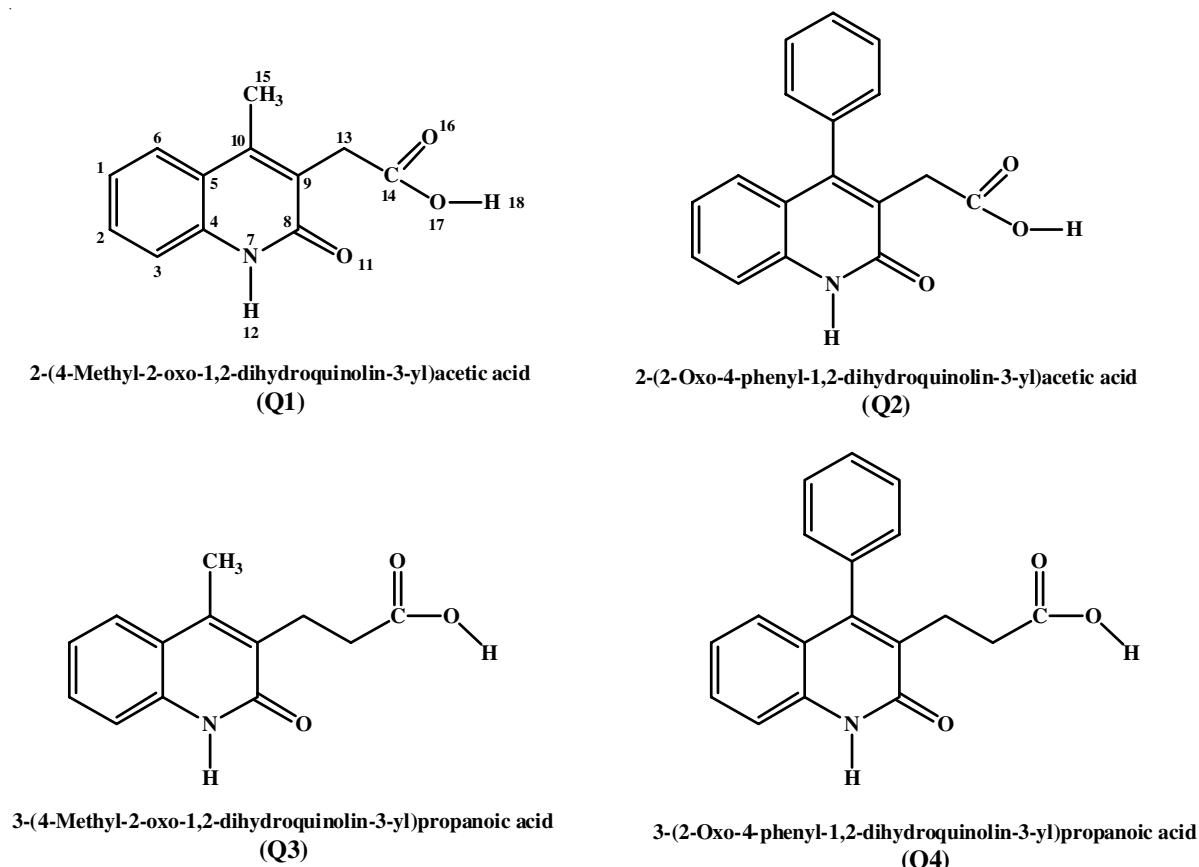


Fig. 1. Structure of quinoline acids (Q1-Q4)

EXPERIMENTAL

1,1-Diphenyl-2-picrylhydrazyl (DPPH), methanol, ethanol, dimethyl sulphide, ethylenediaminetetraacetic acid (EDTA), nitro blue tetrazolium (NBT), riboflavin, hydrogen peroxide, ammonium persulphate, 2,2'-casino-bis-3-ethylbenzothiazoline-6-sulphonic acid (ABTS), sodium phosphate dibasic heptahydrate, sodium phosphate monobasic monohydrate, sodium hydroxide, hydrochloric acid, ascorbic acid and butylated hydroxy anisole were purchased from Sigma-Aldrich, USA.

The studied quinoline derivatives (Q1-Q4) to scavenge the DPPH radical is determined by Hatano *et al.*'s method [21]. The capacity of compounds to scavenge hydrogen peroxide is determined by Ruch *et al.*'s method [22], while the scavenge superoxide is determined by using Winterbourn *et al.*'s method [23]. The ABTS^{•+} radical scavenging activity is done according to the method as described by Shirwaikar *et al.* [24].

The DPPH, hydroxyl, ABTS and superoxide scavenging activities were calculated using the following formulae (1-2):

$$\text{Scavenging activity (\%)} = \frac{A_{\text{control}} - A_{\text{sample}}}{A_{\text{control}}} \times 100$$

$$\text{Superoxide scavenging (\%)} = \frac{A_{\text{After illumination}} - A_{\text{Before illumination}}}{A_{\text{control}}} \times 100$$

Computational studies: The computational analysis was carried out using Gaussian software and the basis set used is density functional theory, B3LYP/6-311G++(d,p) [25-27]. The

calculated gas-phase enthalpy of proton H (H⁺) was 6.197 kJ mol⁻¹ and gas-phase enthalpy of electron H(e) = 3.145 kJ mol⁻¹ from the literature [28,29]. The following quantities bond dissociation energy (BDE), ionization potential (IP) and proton dissociation energy (PDE) can be derived from the calculated total enthalpies at 298.15 K and gas phase.

$$\text{BDE} = H^{(\text{QX}^{\bullet})} + H^{(\text{H}^{\bullet})} - H^{(\text{QX-H})}$$

where QX[•] = enthalpy of radical; H[•] = enthalpy of hydrogen atom; QX-H = enthalpy of neutral molecule; and X = O & N.

$$\text{IP} = H^{(\text{QXH}^{\bullet+})} - H^{(\text{QXH})}$$

$$\text{PDE} = H^{(\text{QX}^{\bullet})} + H^{(\text{H}^{\bullet})} - H^{(\text{QXH}^{\bullet+})}$$

where QXH^{•+} = enthalpy of radical cation; H[•] = enthalpy of hydrogen atom; QX-H = enthalpy of neutral molecule; and X = O & N.

RESULTS AND DISCUSSION

In vitro antioxidant activity: To evaluate the free radical scavenging activity of quinoline acids (Q1-Q4), *in vitro* DPPH, ABTS, superoxide and hydroxyl scavenging methods were performed. The DPPH and ABTS assays were frequently employed method for evaluating the antioxidant activity [30]. The DPPH assay was performed under 50% ethanol/water, while the ABTS assay was carried out in aqueous conditions.

The methodology relies on the observation that a stable free radical (X) can be removed from antioxidants by hydrogen abstraction, and the reaction can be described as follows:



The rate of the reaction was measured in terms of decrease in the X^* concentration, which is related to the ability of trapping of free radicals by the added compounds (YH). A decrease in the intensity of the free radical's solution due to scavenging of free radical by antioxidant molecules was measured colourimetrically at a specific wavelength [31]. Free radical scavenging is the recognized mechanism for antioxidants inhibiting lipid oxidation [32]. For DPPH and ABTS methods, ascorbic acid was used as standard and for hydroxy and superoxide radical scavenging activity, butylated hydroxy anisole was used as reference.

DPPH free radical scavenging assay: The DPPH radical reduces hydrazine when strong hydrogen donors for antioxidants are present, altering the reaction colour from violet to yellow. This change takes place because DPPH radicals can reduce the concentration of hydrazine [28]. All the compounds exhibited a strong to good scavenging activity (Table-1). Compound Q1 demonstrates a potent ability to inhibit DPPH, as seen by the high percentage inhibition value (83%) and the dosage of 58.01 $\mu\text{g}/\text{mL}$ was necessary to achieve a 50% reduction in DPPH. The standard ascorbic acid reduces DPPH at $\text{IC}_{50} = 11.7 \mu\text{g}/\text{mL}$. The radical scavenging activity of the compounds Q1, Q2, Q3 and Q4 at different concentrations is shown in Fig. 2.

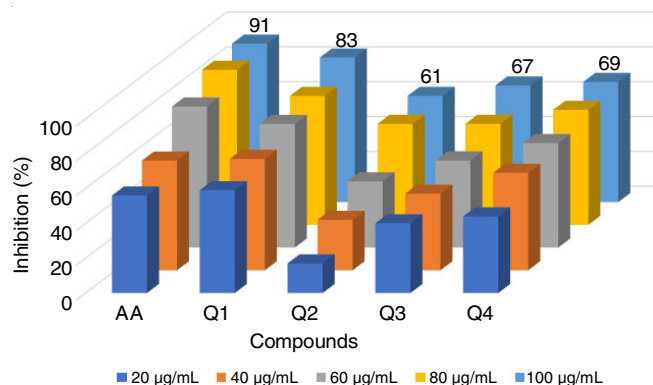


Fig. 2. DPPH radical scavenging ability of the compounds

ABTS cation radical scavenging activity: ABTS is effective for measuring the antioxidant activity of samples in different medium, since it is soluble in both aqueous and organic solvents. It is employed in solutions that replicate an ionic serum with a pH of 7.4 and are based on a phosphate buffer (PBS) that contains 150 mM of NaCl [33]. Compounds Q1 and Q4 have greater inhibitory percentage of (72%; $\text{IC}_{50} = 41 \mu\text{g}/\text{mL}$ and

71%; $\text{IC}_{50} = 42.6 \mu\text{g}/\text{mL}$), whereas ascorbic acid inhibits ABTS as 92%; $\text{IC}_{50} = 12.3 \mu\text{g}/\text{mL}$) ABTS^{•+} scavenging activity compared with compounds Q3 and Q2. The results concludes that inhibitory power of ABTS cation in the order ascorbic acid > Q4 > Q1 > Q3 > Q2 and it is illustrated in Fig. 3. The strong to good results of the ABTS inhibition and DPPH radical scavenging inhibition demonstrates the involvement of either OH or NH or both hydrogen from the compounds [34,35].

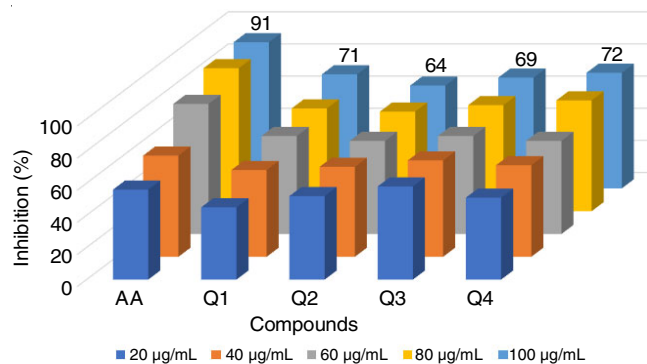


Fig. 3. ABTS inhibition activity of the compounds

Hydroxyl free radical scavenging activity: This assay illustrates the ability of the compounds and standard BHA to inhibit hydroxyl radical produced by Fe^{3+} -EDTA-ascorbate and H_2O_2 . Hydroxyl radicals generated by the Fenton's reaction attack deoxyribose and divide into fragments and reacts with thiobarbituric acid (TBA). This on heating forms pink colour, which is estimated colourimetrically. Ability of the compounds to scavenge hydroxyl radical (OH^*) is directly related to its antioxidant activity [36]. Hydroxyl radical scavenging efficiency of compounds Q1-Q4 is depicted in Fig. 4 and ranges from 72% to 64%. The IC_{50} values of compounds Q1-Q4 are in the range of 40.6-57.3 $\mu\text{g}/\text{mL}$ as indicated in Table-1.

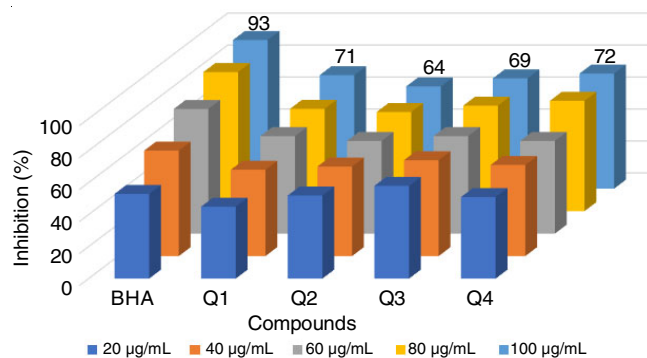


Fig. 4. Hydroxyl scavenging activity

TABLE-1
INHIBITORY CONCENTRATION (IC_{50}) OF QUINOLINE ANTIOXIDANTS IN *in vitro* ANALYSIS

Compounds	DPPH scavenging activity IC_{50} ($\mu\text{g}/\text{mL}$)	ABTS scavenging activity IC_{50} ($\mu\text{g}/\text{mL}$)	Hydroxyl scavenging activity IC_{50} ($\mu\text{g}/\text{mL}$)	Superoxide scavenging activity IC_{50} ($\mu\text{g}/\text{mL}$)
Q1	58.01	41	40.6	8.48
Q2	5.08	49.9	49.25	3.55
Q3	31.75	57.3	57.3	9.35
Q4	43.41	47.6	47.64	7.45
Ascorbic acid	11.7	12.3	–	–
Butylated hydroxy anisole	–	–	14.8	17.5

Superoxide free radical scavenging activity: Superoxide radical scavenging activity is based on the anion radical associated with the PMS-NADH system. The measurement of superoxide scavenging activity is done by the method described by Liu *et al.* [37]. In this method, blue formazan produced by the reduction of yellow dye (NBT) by the superoxide anion is measured spectrophotometrically at 560 nm. In present study, compound Q2 exhibits greater superoxide scavenging activity 66% than others and BHA standard exhibit 88%. Compounds Q1, Q3 and Q4 showed the moderate superoxide scavenging activity (Fig. 5). Compounds Q1-Q4 inhibit 50% of superoxide radical with lower concentration (IC_{50} = 8.48, 3.55, 9.35 and 7.45 $\mu\text{g/mL}$) than standard BHA's IC_{50} found to be 17.5 $\mu\text{g/mL}$.

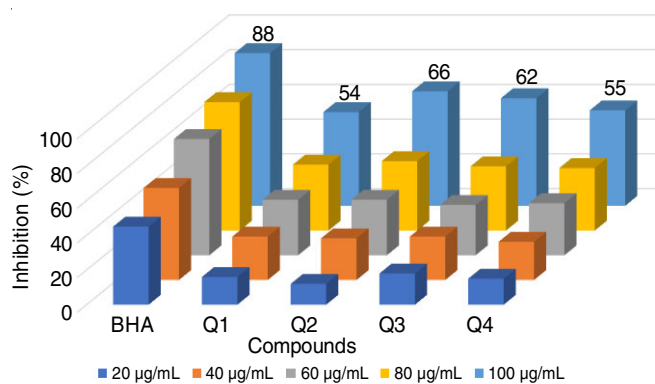


Fig. 5. Superoxide inhibiting activity

Computational analysis: To analyze and evaluate the mechanism of antioxidant potential of the studied compounds HOMO-LUMO, MEP, NPA, BDE, IP, PDE NBO and spin density distributions are computed by DFT method using Gaussian software [38].

Frontier molecular orbital (HOMO-LUMO) analysis: Compounds with lower HOMO energy are weak electron donors and the compounds with higher HOMO energy are good electron donor and thus will act as good antioxidant [39]. Fujishima *et al.* [40] reported that the molecules with large GAP, will have high thermodynamic stability, whereas the molecules with lesser GAP will have an electronic transition [40]. All the studied quinoline acids Q1, Q2, Q3 and Q4 possessed higher HOMO energies and also had lowest gap specifying their antioxidant potential (Fig. 6).

Molecular electrostatic potential map (MEP) and natural population distribution analysis (NPA): Exploring the charge density, MEP diagrams are essentially 3D images of the molecules. In an MEP diagram, red represents electron-rich sites (electrophilic assault) and blue represents electron-poor sites (nucleophilic attack) [41,42]. Hence, more positive charge density site in a molecule will be denoted by dark blue colour, indicating the attack of negatively charged groups such as oxygen free radicals [43]. Analysis of MEP diagram Fig. 7 of compounds Q1, Q2, Q3 and Q4 showed dark blue colour at N-H in B ring of all the studied quinolines. This reflects the fact that N-H group act as electrophilic centre for the attack of

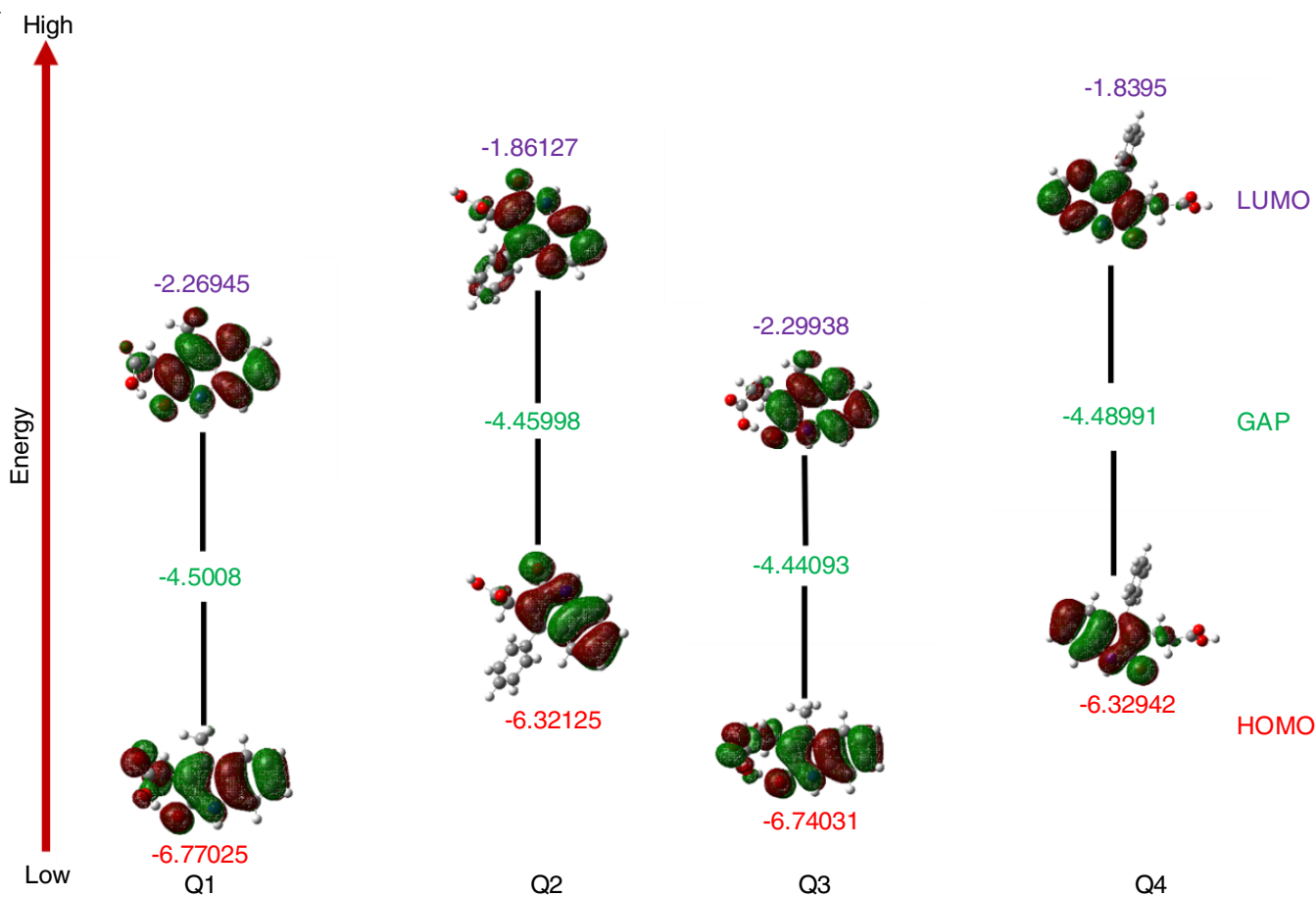


Fig. 6. HOMO-LUMO energies of quinoline acids

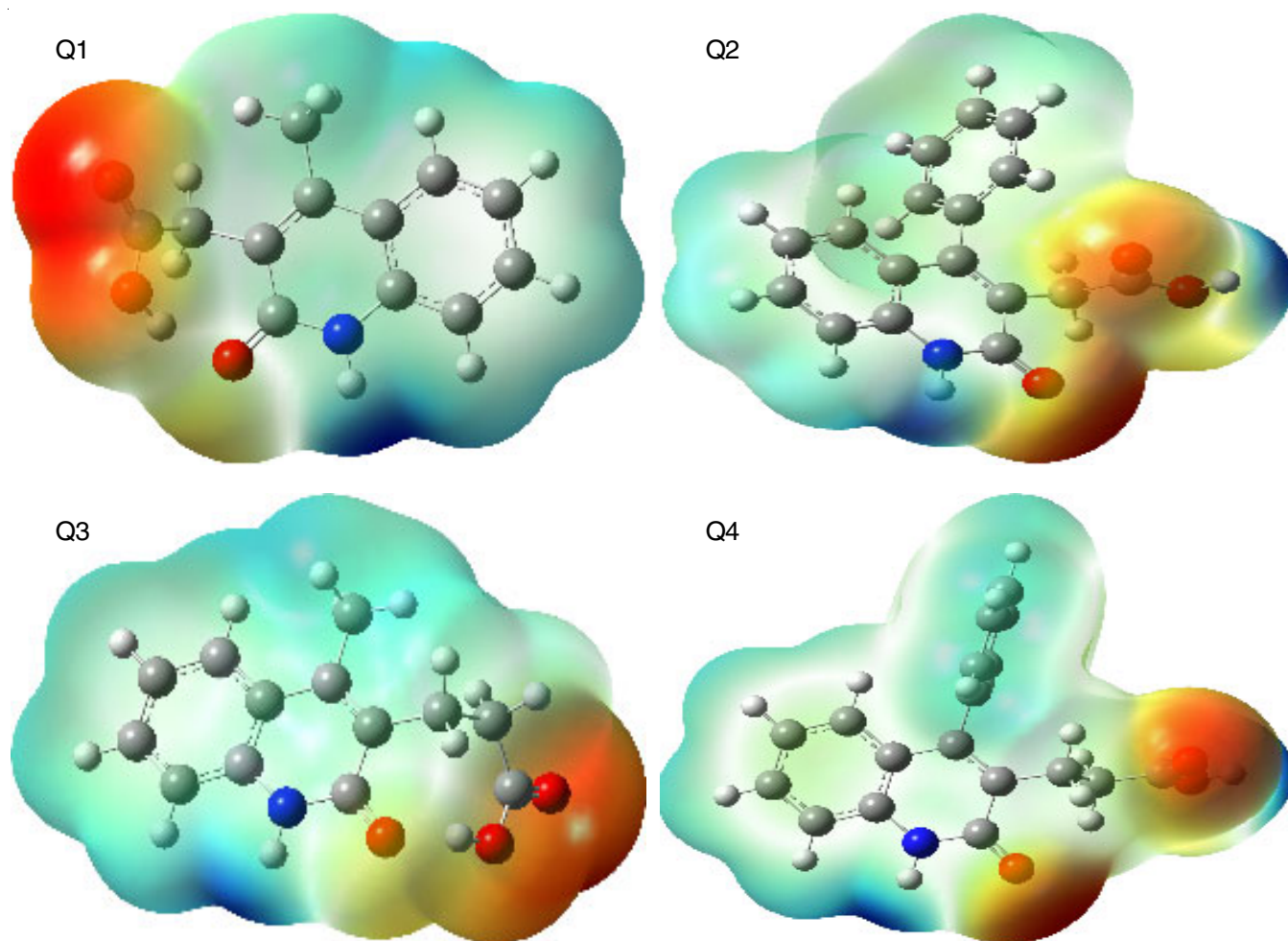


Fig. 7. Molecular electrostatic potential map of quinoline acids

free radicals. Natural population distribution analysis (NPA) depicts more negative charge on oxygen heteroatom (Table-2) at C-14 than on nitrogen atom at C-8 position [44], which is in accordance with MEP analysis. These results are preliminary and further confirmation on the antioxidant potential and mechanism of the radical scavenging activity is done by spin distribution, BDE, IP and PDE analysis.

TABLE-2
NATURAL POPULATION ANALYSIS (NPA) OF OXYGEN
AND NITROGEN ATOMS IN QUINOLINE ACIDS

Compound	NPA of oxygen	NPA of nitrogen
Q1	-0.71992 e	-0.58475 e
Q2	-0.71287 e	-0.59704 e
Q3	-0.72187 e	-0.58424 e
Q4	-0.59484 e	-0.59839 e

Antioxidant mechanism

Hydrogen atom transfer (HAT) mechanism analysis:

To evaluate the antioxidant activity of the studied compounds *via* hydrogen donating mechanism the N-H (ring) and O-H (COOH) homolytic bond dissociation energies (BDE) were computed and taken into account [45]. Since, BDE directly relates to the hydrogen donating ability of the molecules and serves as a significant descriptor for assessing the antioxidant

mechanism by HAT mechanism (Fig. 8). The lowest BDE value of a compound defines the easier hydrogen abstraction ability and thus enhanced radical scavenging ability of the compound [46,47]. From Table-3, it is obvious that compound Q1 has least BDE value 9.38 kJ/mol for the abstraction of hydrogen at -OH site and next lower energy is for Q4 99.90 kJ/mol (N-H). The order of radical scavenging activity is Q1 > Q2 > Q3 > Q4, which is in accordance with the observed experimental results.

TABLE-3
BOND DISSOCIATION ENERGY VALUES AT POSSIBLE SITES

Compound	Bond dissociation energy (kJ mol ⁻¹)	
	O-H	N-H
Q1	9.38	619.51
Q2	758.99	785.69
Q3	634.55	651.66
Q4	892.58	99.90

Sequential electron transfer-proton transfer (SET-PT) mechanism:

The second mechanism by which an antioxidant act through is SET-PT route. In two-step mechanism involved in this process, first step the compound becomes radical cation by donating electron to the free radical, which depicted in Fig. 9 [47,48]. This is characterized by ionization (IP) values, which illustrates the electron transfer ability and serves as an

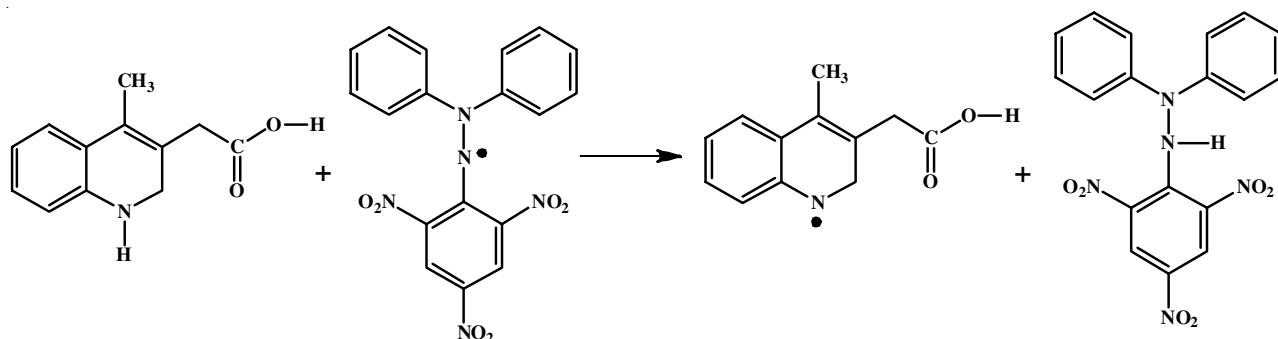


Fig. 8. Bond dissociation energy mechanism of quinoline acid (Q1)

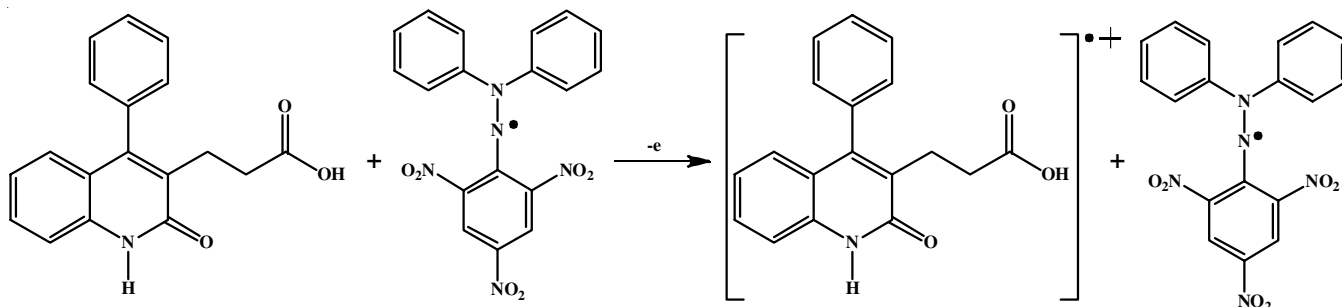


Fig. 9. STEP 1 - Sequential electron transfer (SET)

important parameter for studying the antioxidant mechanism. The higher the value of IP, the more difficult is to remove an electron from the molecule.

The second step is the deprotonation step, which is demonstrated by proton dissociation enthalpy (PDE) values (Fig. 10). The IP and PDE values for the studied compounds are presented in Table-4 and this indicates the lower IP and PDE values for compound Q4 *viz.* 212.62 kJ mol⁻¹ and 321.89 kJ mol⁻¹ (N-H), respectively. The PDE value of compound Q4 is greater than BDE value demonstrating the occurrence SET-PT mechanism. Also, both PDE and BDE values for N-H is lesser than for O-H

for compound Q4 signifying the contribution of N-H proton for the radical scavenging activity and the O-H plays a less significant role. For other compounds, the values are higher hence SET-PT mechanism may not be feasible.

Spin density analysis: Stability of the free radical formed is represented by spin density parameter. If spin density is more delocalized in the radical, the radical will be easily formed and its BDE will be lesser consequently greater antioxidant activity [27,49]. Hence, the assessment of spin densities of the radicals both for N[•] and O[•] formed for the studied compounds are carried out to rationalize the reactivity at N-H and O-H site and are shown in Fig. 11. Analysis of the spin densities of the compounds shows extended delocalization of the radical species on all the aromatic rings for all studied compounds. The spin densities of 'O' atoms of O-H radicals were 0.8180, 0.5728, 0.55202 and 0.2998, respectively for compounds Q1, Q2, Q3 and Q4 (Table-5). Similarly, for 'N' atoms of the N-H radicals were 0.7250, 0.707605, 0.6186 and 0.000523 respectively for compounds Q1, Q2, Q3 and Q4, which suggests the stabilization of both the N[•] and O[•] radicals in the order Q1 > Q2 > Q3 > Q4. The radical formed from compound Q1 is

Compound	Ionization potential (kJ mol ⁻¹)	Proton dissociation energy (kJ mol ⁻¹)	
		O-H	N-H
		Q1	805.34
Q2	971.52	1054.10	1080.80
Q3	834.59	929.66	946.86
Q4	212.62	1187.88	321.89

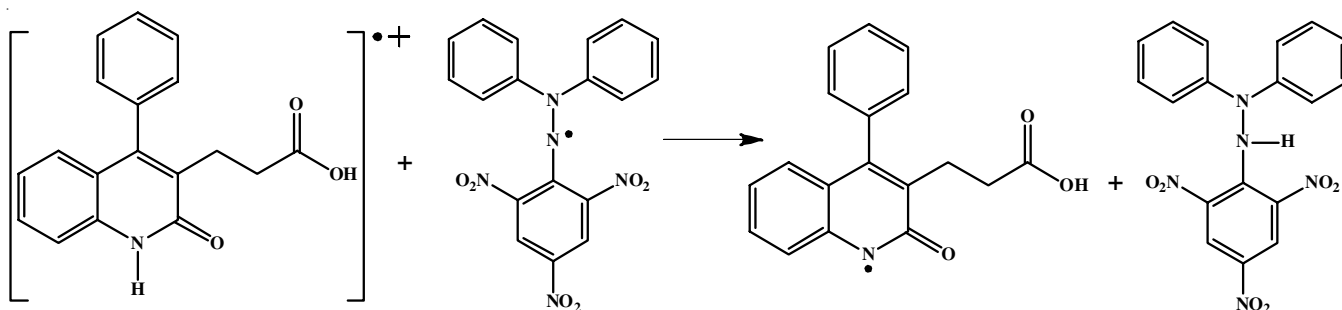


Fig. 10. STEP 2 - Proton transfer (PT)

TABLE-5
SPIN DENSITY DISTRIBUTION OF QUINOLINE ACIDS

Compound	N-H	O-H
Q1	<p>Spin density values for Q1 (N-H): -0.023880 (CH₃), 0.072653, -0.048891, 0.092866, 0.004736, -0.003602 (C=O), 0.003397, 0.000262 (O-H), -0.007875, 0.085809, 0.009501, 0.022793, -0.031625, -0.000587, 0.093213, 0.725026 (N), -0.049512, 0.080452, 0.089421, -0.012503, -0.023914, 0.085985, -0.001509, 0.003534, 0.011098, 0.007580, 0.0118914 (C=O), 0.006459, -0.034491, -0.001550, 0.005057, -0.000868, 0.007425, 0.707605, -0.000955, 0.000181, 0.000318, 0.000955 (O-H).</p>	<p>Spin density values for Q1 (O-H): 0.004109 (CH₃), 0.006330, 0.001518, 0.000312, -0.039198, 0.818064 (O), 0.001415 (C=O), 0.000874, 0.003259, 0.012608, -0.004434, 0.012608, 0.009419, 0.023682, -0.002547, 0.063375, 0.101215, 0.008014, -0.002558, 0.011547, 0.008112, 0.006610, -0.052381, -0.024515, -0.038764, 0.095135, 0.007580, 0.043462 (C=O), 0.074395, -0.005498, -0.009432, 0.063079, 0.065746, 0.008221, 0.005152, 0.190705, 0.572826 (O-H), 0.005445 (CH₃), 0.248405 (C=O), 0.002260, 0.042755 (O-H), 0.012316, 0.007999, 0.007890, 0.022523, -0.001711 (O), -0.001912, 0.038062, -0.004821, 0.552026 (O-H), 0.013020, -0.031949, 0.019414, 0.140695, 0.003258, 0.013863, 0.001835, -0.004167, 0.006717, 0.015678, 0.608630 (C=O), 0.024011, -0.024976, -0.013495, 0.023451, 0.026176, -0.010148, 0.001229 (O-H), 0.006067, 0.121611, 0.004891, 0.288853 (O-H), 0.086058 (O-H), 0.005079, -0.097718, 0.488346, 0.001977, 0.009373, -0.006620, 0.005223, 0.04198, 0.006707, 0.008638, -0.001409, 0.038421, 0.000578, 0.038108, -0.000891, 0.299841 (O-H), -0.001669, 0.013873, 0.001434, -0.00014, 0.005348, -0.003179, 0.013873, 0.001434, -0.00014, 0.005348.</p>
Q2	<p>Spin density values for Q2 (N-H): -0.018591 (CH₃), 0.053860, -0.037410, 0.077283, 0.006608, 0.002260, 0.042755 (O-H), 0.001751, 0.065388, 0.049650, -0.006103, 0.618692 (N), 0.002120, -0.011587, -0.013448, 0.090098, 0.024011, -0.024976, -0.013495, 0.023451, 0.026176, -0.010148, 0.001229 (O-H), 0.006067, 0.121611, 0.004891, 0.288853 (O-H), 0.086058 (O-H), 0.005079, -0.097718, 0.488346, 0.001977, 0.009373, -0.006620, 0.005223, 0.04198, 0.006707, 0.008638, -0.001409, 0.038421, 0.000578, 0.038108, -0.000891, 0.299841 (O-H), -0.001669, 0.013873, 0.001434, -0.00014, 0.005348, -0.003179, 0.013873, 0.001434, -0.00014, 0.005348.</p>	<p>Spin density values for Q2 (O-H): 0.008014, -0.002558, 0.011547, 0.008112, 0.006610, -0.052381, -0.024515, -0.038764, 0.095135, 0.007580, 0.043462 (C=O), 0.074395, -0.005498, -0.009432, 0.063079, 0.065746, 0.008221, 0.005152, 0.190705, 0.572826 (O-H), 0.005445 (CH₃), 0.248405 (C=O), 0.002260, 0.042755 (O-H), 0.012316, 0.007999, 0.007890, 0.022523, -0.001711 (O), -0.001912, 0.038062, -0.004821, 0.552026 (O-H), 0.013020, -0.031949, 0.019414, 0.140695, 0.003258, 0.013863, 0.001835, -0.004167, 0.006717, 0.015678, 0.608630 (C=O), 0.024011, -0.024976, -0.013495, 0.023451, 0.026176, -0.010148, 0.001229 (O-H), 0.006067, 0.121611, 0.004891, 0.288853 (O-H), 0.086058 (O-H), 0.005079, -0.097718, 0.488346, 0.001977, 0.009373, -0.006620, 0.005223, 0.04198, 0.006707, 0.008638, -0.001409, 0.038421, 0.000578, 0.038108, -0.000891, 0.299841 (O-H), -0.001669, 0.013873, 0.001434, -0.00014, 0.005348, -0.003179, 0.013873, 0.001434, -0.00014, 0.005348.</p>
Q3	<p>Spin density values for Q3 (N-H): -0.018591 (CH₃), 0.053860, -0.037410, 0.077283, 0.006608, 0.002260, 0.042755 (O-H), 0.001751, 0.065388, 0.049650, -0.006103, 0.618692 (N), 0.002120, -0.011587, -0.013448, 0.090098, 0.024011, -0.024976, -0.013495, 0.023451, 0.026176, -0.010148, 0.001229 (O-H), 0.006067, 0.121611, 0.004891, 0.288853 (O-H), 0.086058 (O-H), 0.005079, -0.097718, 0.488346, 0.001977, 0.009373, -0.006620, 0.005223, 0.04198, 0.006707, 0.008638, -0.001409, 0.038421, 0.000578, 0.038108, -0.000891, 0.299841 (O-H), -0.001669, 0.013873, 0.001434, -0.00014, 0.005348, -0.003179, 0.013873, 0.001434, -0.00014, 0.005348.</p>	<p>Spin density values for Q3 (O-H): 0.008014, -0.002558, 0.011547, 0.008112, 0.006610, -0.052381, -0.024515, -0.038764, 0.095135, 0.007580, 0.043462 (C=O), 0.074395, -0.005498, -0.009432, 0.063079, 0.065746, 0.008221, 0.005152, 0.190705, 0.572826 (O-H), 0.005445 (CH₃), 0.248405 (C=O), 0.002260, 0.042755 (O-H), 0.012316, 0.007999, 0.007890, 0.022523, -0.001711 (O), -0.001912, 0.038062, -0.004821, 0.552026 (O-H), 0.013020, -0.031949, 0.019414, 0.140695, 0.003258, 0.013863, 0.001835, -0.004167, 0.006717, 0.015678, 0.608630 (C=O), 0.024011, -0.024976, -0.013495, 0.023451, 0.026176, -0.010148, 0.001229 (O-H), 0.006067, 0.121611, 0.004891, 0.288853 (O-H), 0.086058 (O-H), 0.005079, -0.097718, 0.488346, 0.001977, 0.009373, -0.006620, 0.005223, 0.04198, 0.006707, 0.008638, -0.001409, 0.038421, 0.000578, 0.038108, -0.000891, 0.299841 (O-H), -0.001669, 0.013873, 0.001434, -0.00014, 0.005348, -0.003179, 0.013873, 0.001434, -0.00014, 0.005348.</p>
Q4	<p>Spin density values for Q4 (N-H): -0.018591 (CH₃), 0.053860, -0.037410, 0.077283, 0.006608, 0.002260, 0.042755 (O-H), 0.001751, 0.065388, 0.049650, -0.006103, 0.618692 (N), 0.002120, -0.011587, -0.013448, 0.090098, 0.024011, -0.024976, -0.013495, 0.023451, 0.026176, -0.010148, 0.001229 (O-H), 0.006067, 0.121611, 0.004891, 0.288853 (O-H), 0.086058 (O-H), 0.005079, -0.097718, 0.488346, 0.001977, 0.009373, -0.006620, 0.005223, 0.04198, 0.006707, 0.008638, -0.001409, 0.038421, 0.000578, 0.038108, -0.000891, 0.299841 (O-H), -0.001669, 0.013873, 0.001434, -0.00014, 0.005348, -0.003179, 0.013873, 0.001434, -0.00014, 0.005348.</p>	<p>Spin density values for Q4 (O-H): 0.008014, -0.002558, 0.011547, 0.008112, 0.006610, -0.052381, -0.024515, -0.038764, 0.095135, 0.007580, 0.043462 (C=O), 0.074395, -0.005498, -0.009432, 0.063079, 0.065746, 0.008221, 0.005152, 0.190705, 0.572826 (O-H), 0.005445 (CH₃), 0.248405 (C=O), 0.002260, 0.042755 (O-H), 0.012316, 0.007999, 0.007890, 0.022523, -0.001711 (O), -0.001912, 0.038062, -0.004821, 0.552026 (O-H), 0.013020, -0.031949, 0.019414, 0.140695, 0.003258, 0.013863, 0.001835, -0.004167, 0.006717, 0.015678, 0.608630 (C=O), 0.024011, -0.024976, -0.013495, 0.023451, 0.026176, -0.010148, 0.001229 (O-H), 0.006067, 0.121611, 0.004891, 0.288853 (O-H), 0.086058 (O-H), 0.005079, -0.097718, 0.488346, 0.001977, 0.009373, -0.006620, 0.005223, 0.04198, 0.006707, 0.008638, -0.001409, 0.038421, 0.000578, 0.038108, -0.000891, 0.299841 (O-H), -0.001669, 0.013873, 0.001434, -0.00014, 0.005348, -0.003179, 0.013873, 0.001434, -0.00014, 0.005348.</p>

more stabilized, which also has lower BDE values suggesting the enhanced activity of compound Q1, which also correlates with experimental results.

Natural bond orbital (NBO) analysis: The natural bond orbital (NBO) analysis for the studied compounds Q1, Q2, Q3 and Q4 were carried out to investigate the hyper conjugative interactions in the compounds and the obtained perturbation energy (E^2) values are given in Table-6. These hyperconjugative interactions in terms of E^2 values are the measure of intramolecular delocalization [50]. Strong interaction between the electron

donor and acceptors in the molecular system is represented by the larger E^2 values, which consequently demonstrates the effective conjugation in the molecule [51]. The NBO analysis revealed the stronger delocalization through intramolecular hyperconjugation in the compounds. For compounds Q1 and Q3, the greater stabilization energies 294.34 and 289.08 kcal mol⁻¹ comes from the electron donating ability of 'C' lone pair centre $C_4(LP1)-\sigma^*C_3-N_{19}$ and $C_4(LP1)-\sigma^*C_3-N_{15}$, respectively. For compounds Q2 and Q4 more stabilization arises from $\pi^*C_2-C_3$ to $\pi^*C_4-C_5$ for both molecules with energies 296.46

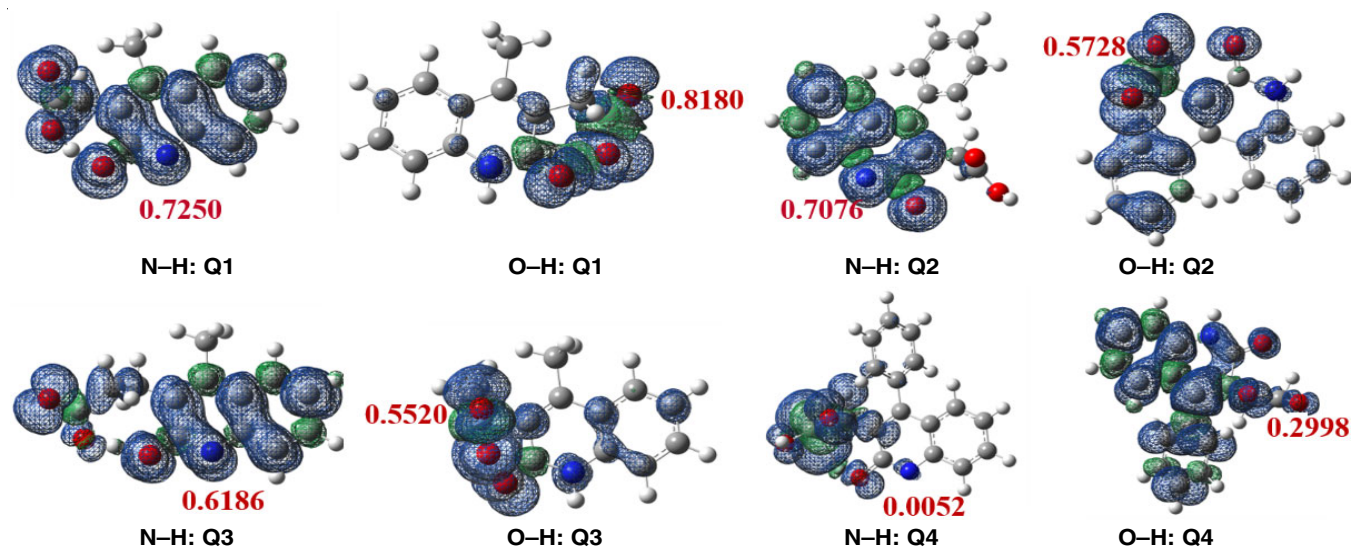


Fig. 11. Delocalization of spin density distribution

TABLE-6							
NBO ANALYSIS (SECOND ORDER PERTURBATION THEORY (FOCK MATRIX) ANALYSIS)							
Compound	Donor	Type	ED of donor	Acceptor	Type	ED of acceptor	E ² (kcal/mol)
Q1	C1-C2	π	1.97741	C3-N19	π^*	0.75874	35.12
	C3-N19	π	1.98515	C13-O20	π^*	0.42749	34.48
	C5-C6	π	1.97962	C4	LP	0.00544	43.27
	C5-C6	π	1.97962	C1-C2	π^*	0.30714	21.08
	C11-C12	π	1.97417	C4	LP	0.00544	29.25
	C11-C12	π	1.99846	C13-O20	π^*	0.42749	27.20
	C4	LP (1)	1.05232	C3-N19	σ^*	0.75874	294.34
	C4	LP (1)	1.05232	C5-C6	σ^*	0.29142	60.98
	C4	LP (1)	1.05232	C11-C12	σ^*	0.19545	49.10
	O20	LP (2)	1.96436	C12-C13	σ^*	0.05747	13.23
	O20	LP (2)	1.96436	C 13 - N 19	σ^*	0.06997	25.80
	O20	LP (2)	1.96436	O 26 - H 27	σ^*	0.05967	14.30
	O25	LP (2)	1.99960	C15	RY	0.01724	19.94
	O25	LP (2)	1.99960	C15-O26	σ^*	0.09594	34.81
	O26	LP (2)	1.99963	C15-C25	σ^*	0.23496	56.08
	C3-N19	π^*	1.98515	C1-C2	π^*	0.01451	69.65
	C3-N19	π^*	1.98515	C13-C20	π^*	0.42749	75.16
C13-O20	π^*	1.99415	C11-C12	π^*	0.19545	45.24	
Q2	C1-C6	π	1.97939	C4-C5	π^*	0.41694	23.78
	C2-C3	π	1.97450	C1-C6	π^*	0.37965	23.29
	C4-C5	π	1.97170	C2-C3	π^*	0.37965	23.57
	C11-C12	π	1.97077	C13-O21	π^*	0.37107	23.22
	C22-C24	π	1.96971	C23-C25	π^*	0.32743	20.49
	C22-C24	π	1.96971	C27-C29	π^*	0.32700	19.81
	C23-C25	π	1.97832	C22-C24	π^*	0.34905	20.24
	C23-C25	π	1.97832	C27-C29	π^*	0.32700	20.01
	C27-C29	π	1.98016	C22-C24	π^*	0.34905	20.64
	C-27-C29	π	1.98016	C23-C25	π^*	0.32743	20.44
	O16	LP (2)	1.8463	C14-C15	σ^*	0.07159	36.86
	N20	LP (1)	1.99889	C15-C34	σ^*	0.10556	44.17
	N20	LP (1)	1.99889	C2-C3	σ^*	0.41695	60.66
	O21	LP (1)	1.81452	C13-N20	σ^*	0.08058	28.32
	O34	LP (2)	1.81452	C15-O16	σ^*	0.22161	50.01
	C2-C3	π^*	1.97450	C1-C6	π^*	0.37965	280.40
	C2-C3	π^*	1.97450	C4-C5	π^*	0.41694	296.46
C4-C5	π^*	1.97170	C11-C12	π^*	0.17595	100.37	
C13-O21	π^*	1.99439	C11-C12	π^*	0.17595	52.47	

Q3	C1-C2	π	1.97743	C3-N15	π^*	0.75547	34.98
	C11-C12	π	1.97432	C4	LP	0.00547	29.80
	C11-C12	π	1.97432	C13-O16	π^*	0.42566	26.58
	C4	LP (1)	1.99843	C3-N15	σ^*	0.75547	289.08
	C4	LP (1)	1.99843	C5-C6	σ^*	0.29354	61.34
	C4	LP (1)	1.99843	C11-C12	σ^*	0.18771	48.02
	O28	LP (2)	1.99960	C27-O29	σ^*	0.09720	34.43
	C3-N15	π^*	1.98522	C1-C2	π^*	0.30647	70.06
	C3-N15	π^*	1.98522	C13-O16	π^*	0.42566	69.51
	C13-O16	π^*	1.99409	C11-C12	π^*	0.18771	47.45
	C27-O28	π^*	1.99382	C27-O29	π^*	0.09720	45.47
	Q4	C1-C6	π	1.97937	C4-C5	π^*	0.41731
C2-C3		π	1.97447	C1-C6	π^*	0.38016	23.13
C4-C5		π	1.97158	C2-C3	π^*	0.41844	23.55
N15		LP (1)	1.60978	C2-C3	σ^*	0.41844	44.04
N15		LP (1)	1.60978	C13-O16	σ^*	0.37409	60.82
O16		LP (2)	1.86705	C13-N15	σ^*	0.08087	28.19
O34		LP (1)	1.97462	C35-O36	σ^*	0.22110	49.10
O36		LP (2)	1.97432	O34-C35	σ^*	0.02667	37.64
C2-C3		π^*	1.97447	C1-C6	π^*	0.38016	278.09
C2-C3		π^*	1.97447	C4-C5	π^*	0.41731	289.21
C4-C5		π^*	1.97158	C11-C12	π^*	0.17340	98.66
C13-O16		π^*	1.99437	C11-C12	π^*	0.17340	50.25

E² = Energy of hyper conjugation interaction (Stabilization energy), LP = lone pair electrons, σ and π -Bonding orbitals, σ^ and π^* -Antibonding orbitals. RY* = Rydberg, ED = Electron density.

and 289.21 kcal mol⁻¹, respectively. Hence, quinoline acids (Q1-Q4) possess high stability and hence has more antioxidant potential.

Conclusion

Four quinoline acid derivatives (Q1-Q4) were tested for their ability to scavenge free radicals *in vitro* using the DPPH, ABTS, H₂O₂ and superoxide radical assays. Compound Q1 demonstrated the potent antioxidant in DPPH radical scavenging activity. The obtained results revealed that compound Q4 exhibits effective scavenging activity in ABTS and hydrogen peroxide. The superoxide radical scavenging results showed that compound Q2 exhibit good radical quenching capacity. Structure-based antioxidant property in gas phase was also calculated using DFT/B3LYP/6-311++(d,p) level of theory in this study. Quinoline acids (Q1-Q4) demonstrated high HOMO energies and had low GAP, indicating a high antioxidant potential. Based on electrostatic potential map (MEP), natural population distribution analysis (NPA) and natural bond orbital analyses (NBO), nitrogen appears to be the most powerful radical attacking site. According to the bond dissociation energies (BDE) results, compound Q1 exhibits low bond dissociation energy in the O-H radical, which suggests that it follows the HAT mechanism. The N-H radical in Q4 molecule evidently follows the SET-PT mechanism due to the lower value of PDE and BDE than O-H radical. The analysis of the spin distributions of N[•] and O[•] revealed a stabilization order of Q1 > Q2 > Q3 > Q4.

CONFLICT OF INTEREST

The authors declare that there is no conflict of interests regarding the publication of this article.

REFERENCES

1. A. Thyagarajan and R.P. Sahu, *Integr. Cancer Ther.*, **17**, 210 (2018); <https://doi.org/10.1177/1534735416681639>
2. W. Si, Y.P. Chen, J. Zhang, Z.-Y. Chen and H.Y. Chung, *Food Chem.*, **239**, 1117 (2018); <https://doi.org/10.1016/j.foodchem.2017.07.055>
3. A. Lozynskyi, V. Zasadko, D. Atamanyuk, D. Kaminsky, H. Derkach, O. Karpenko, V. Ogurtsov, R. Kutsyk and R. Lesyk, *Mol. Divers.*, **21**, 427 (2017); <https://doi.org/10.1007/s11030-017-9737-8>
4. Y. Dai, C. Shao, Y. Piao, H. Hu, K. Lu, T. Zhang, X. Zhang, S. Jia, M. Wang and S. Man, *Carbohydr. Polym.*, **178**, 34 (2017); <https://doi.org/10.1016/j.carbpol.2017.09.016>
5. R.P. Mason, *Redox Biol.*, **8**, 422 (2016); <https://doi.org/10.1016/j.redox.2016.04.003>
6. M.J. Engelhart, M.I. Geerlings, A. Ruitenbergh, J.C. van Swieten, A. Hofman, J.C.M. Witteman and M.M.B. Breteler, *JAMA*, **24**, 3223 (2002); <https://doi.org/10.1001/jama.287.24.3223>
7. S.B. Christensen, *Biomedicines*, **9**, 472 (2021); <https://doi.org/10.3390/biomedicines9050472>
8. P.Y. Chung, Z.-X. Bian, H.-Y. Pun, D. Chan, A.S.-C. Chan, C.-H. Chui, J.C.-O. Tang and K.-H. Lam, *Future Med. Chem.*, **7**, 947 (2015); <https://doi.org/10.4155/fmc.15.34>
9. B.S. Matada, R. Pattanashettar and N.G. Yernale, *Bioorg. Med. Chem.*, **32**, 115973 (2021); <https://doi.org/10.1016/j.bmc.2020.115973>
10. G. da R.M. Machado, D. Diedrich, T.C. Ruaro, A.R. Zimmer, M.L. Teixeira, L.F. de Oliveira, M. Jean, P. Van de Weghe, S.F. de Andrade, S.C. Baggio-Gnoatto and A.M. Fuentesfria1, *Braz. J. Microbiol.*, **51**, 1691 (2020); <https://doi.org/10.1007/s42770-020-00348-4>
11. B. Abdi, M. Fekadu, D. Zeleke, R. Eswaramoorthy and Y. Melaku, *J. Chem.*, **2021**, 2408006 (2021); <https://doi.org/10.1155/2021/2408006>
12. M.O. Puskullu, H. Shirinzadeh, M. Nenni, H. Gurer-Orhan and S. Suzen, *J. Enzyme Inhib. Med. Chem.*, **31**, 121 (2015); <https://doi.org/10.3109/14756366.2015.1005012>

13. S.R. Prasad, N.D. Satyanarayan, A.S.K. Shetty, H. Shivanna and B. Thippeswamy, *Asian J. Chem.*, **34**, 2067 (2022); <https://doi.org/10.14233/ajchem.2022.23760>
14. M. Brahmaya, *J. Appl. Pharm. Sci.*, **2**, 041 (2012); <https://doi.org/10.7324/JAPS.2012.21008>
15. H. Hemant, L.G. Santosh, P.B. Naveen and S.S. Nitinkumar, *Rasayan J. Chem.*, **13**, 1744 (2020); <https://doi.org/10.31788/RJC.2020.1335669>
16. L. Savegnago, A.I. Vieira, N. Seus, B.S. Goldani, M.R. Castro, E.J. Lenardão and D. Alves, *Tetrahedron Lett.*, **54**, 40 (2013); <https://doi.org/10.1016/j.tetlet.2012.10.067>
17. I. Bazine, Z. Cheraïet, R. Bensegueni, C. Bensouici and A. Boukhari, *J. Heterocycl. Chem.*, **57**, 2139 (2020); <https://doi.org/10.1002/jhet.3933>
18. W. Rogoz, A. Owczarzy, K. Kulig, A. Zieba and M. Macilzek-Jurczyk, *Molecules*, **28**, 320 (2022); <https://doi.org/10.3390/molecules28010320>
19. P. Shanmugam, *Proc. Indian Acad. Sci. Sect. A Phys. Sci.*, **51**, 75 (1960); <https://doi.org/10.1007/BF03048937>
20. J.P. John and P. Shanmugam, *Proc. Indian Acad. Sci. Sect. A Phys. Sci.*, **54**, 161 (1961); <https://doi.org/10.1007/BF03045776>
21. T. Hatano, H. Kagawa, T. Yasuhara and T. Okuda, *Chem. Pharm. Bull. (Tokyo)*, **36**, 2090 (1988); <https://doi.org/10.1248/cpb.36.2090>
22. R.J. Ruch, S.J. Cheng and J.E. Klaunig, *Carcinogenesis*, **10**, 1003 (1989); <https://doi.org/10.1093/carcin/10.6.1003>
23. C.C. Winterbourn, R.E. Hawkins, M. Brian and R.W. Carrell, *J. Lab. Clin. Med.*, **85**, 337 (1975).
24. A. Shirwaikar, A. Shirwaikar, K. Rajendran and I.S.R. Punitha, *Biol. Pharm. Bull.*, **29**, 1906 (2006); <https://doi.org/10.1248/bpb.29.1906>
25. T. Brinck, M. Haeberlein and M. Jonsson, *J. Am. Chem. Soc.*, **119**, 4239 (1997); <https://doi.org/10.1021/ja962931+>
26. J.E. Bartmess, *J. Phys. Chem.*, **98**, 6420 (1994); <https://doi.org/10.1021/j100076a029>
27. J. Rimarèfk, V. Lukes, E. Klein and M. Ilèin, *J. Mol. Struct. THEOCHEM*, **952**, 25 (2010); <https://doi.org/10.1016/j.theochem.2010.04.002>
28. J.R.B. Gomes and F. Illas, *Catal. Lett.*, **71**, 31 (2001); <https://doi.org/10.1023/A:1016644006002>
29. A.C. Olleta and S.I. Lane, *Phys. Chem. Chem. Phys.*, **3**, 811 (2001); <https://doi.org/10.1039/b005375j>
30. P.J. Patel, D.M. Patel, R.M. Vala, D.B. Upadhyay, Y. Pannarselvam, S.G. Patel and H.M. Patel, *ACS Omega*, **8**, 444 (2023); <https://doi.org/10.1021/acsomega.2c05020>
31. S.M. Bayomi, H.A. El-Kashef, M.B. El-Ashmawy, M.N.A. Nasr, M.A. El-Sherbeny, F.A. Badria, L.A. Abou-zeid, M.A. Ghaly and N.I. Abdel-Aziz, *Med. Chem. Res.*, **22**, 1147 (2013); <https://doi.org/10.1007/s00044-012-0116-9>
32. W. Brand-Williams, M.E. Cuvelier and C. Berset, *Lebensm. Wiss. Technol.*, **28**, 25 (1995); [https://doi.org/10.1016/S0023-6438\(95\)80008-5](https://doi.org/10.1016/S0023-6438(95)80008-5)
33. E.A. Shalaby and S.M.M. Shanab, *Indian J. Geo-Mar. Sci.*, **42**, 556 (2013).
34. A. Ismail, Z.M. Marjan and C.W. Foong, *Food Chem.*, **87**, 581 (2004); <https://doi.org/10.1016/j.foodchem.2004.01.010>
35. A. Santiago and R. Malvar, *Int. J. Mol. Sci.*, **11**, 691 (2010); <https://doi.org/10.3390/ijms11020691>
36. K.N. Mohana and C.B.P. Kumar, *ISRN Org. Chem.*, **2013**, 1 (2013); <https://doi.org/10.1155/2013/620718>
37. F. Liu, V.E.C. Ooi and S.T. Chang, *Life Sci.*, **60**, 763 (1997); [https://doi.org/10.1016/S0024-3205\(97\)00004-0](https://doi.org/10.1016/S0024-3205(97)00004-0)
38. M.J. Frisch, G.W. Trucks, H.B. Schlegel, G.E. Scuseria, M.A. Robb, J.R. Cheeseman, G. Scalmani, V. Barone, B. Mennucci, G.A. Petersson, H. Nakatsuji, M. Caricato, X. Li, H.P. Hratchian, A.F. Izmaylov, J. Bloino, G. Zheng, J.L. Sonnenberg, M. Hada, M. Ehara, K. Toyota, R. Fukuda, J. Hasegawa, M. Ishida, T. Nakajima, Y. Honda, O. Kitao, H. Nakai, T. Vreven, J.A. Montgomery, J.E. Peralta, F. Ogliaro, J.J. Heyd, M. Bearpark, E. Brothers, K.N. Kudin, V.N. Staroverov, R. Kobayashi, J. Normand, K. Raghavachari, P.G. Rendell, J.C. Burant, S.S. Iyengar, J. Tomasi, M. Cossi, N. Rega, J.M. Millam, M. Klene, J.E. Knox, J.B. Cross, V. Bakken, C. Adamo, J. Jaramillo, R. Gomperts, R.E. Stratmann, O. Yazyev, A.J. Austin, R. Cammi, C. Pomelli, J.W. Ochterski, R.L. Martin, K. Morokuma, V.G. Zakrzewski, G.A. Voth, P. Salvador, J.J. Dannenberg, S. Dapprich, A.D. Daniels, O. Farkas, J.B. Foresman, J.V. Ortiz, J. Cioslowski and D.J. Fox, *Gaussian 09 Revision D.01* (2014).
39. J.B. Veselinovic, A.M. Veselinovic, Z.J. Vitnik, V.D. Vitnik and G.M. Nikolic, *Chem. Biol. Interact.*, **214**, 49 (2014); <https://doi.org/10.1016/j.cbi.2014.02.010>
40. M.T. Fujishima, N. Silva, R. Ramos, E. Batista Ferreira, K. Santos, C. Silva, J. Silva, J. Campos-Rosa and C. Santos, *Pharmaceuticals*, **11**, 72 (2018); <https://doi.org/10.3390/ph11030072>
41. T.T. Phan and N.T. Son, *J. Mol. Model.*, **27**, 6 (2021); <https://doi.org/10.1007/s00894-020-04639-3>
42. N.T. Son, P.T. Thuy, D.T.M. Thanh and N.V. Trang, *J. Mol. Struct.*, **11224**, 12902 (2021); <https://doi.org/10.1039/d1ra01076j>
43. S.A. de Souza Farias, K.S. da Costa and J.B.L. Martins, *ACS Omega*, **6**, 8908 (2021); <https://doi.org/10.1021/acsomega.0c06156>
44. T. Leila, Q.D. Duy and A.V. Thuy, *RSC Adv.*, **9**, 3320 (2019); <https://doi.org/10.1039/C8RA09763A>
45. V.V. Quan, C.N. Pham, M.T. Nguyen, T.T. Nguyen, D.P. Cam-Tu and M. Adam, *ACS Omega*, **4**, 8935 (2019); <https://doi.org/10.1021/acsomega.9b00677>
46. J.S. Wright, E.R. Johnson and G.A. Di Labio, *J. Am. Chem. Soc.*, **123**, 1173 (2001); <https://doi.org/10.1021/ja002455u>
47. A. Galano and J.R. Alvarez-Idaboy, *J. Comput. Chem.*, **34**, 2430 (2013); <https://doi.org/10.1002/jcc.23409>
48. A. Fassih, F. Hasanzadeh, A.M. Attar, L. Saghale and M. Mohammadpour, *Res. Pharm. Sci.*, **15**, 515 (2020); <https://doi.org/10.4103/1735-5362.301336>
49. N. Zhang, Y. Wu, M. Qiao, W. Yuan, X. Li, X. Wang, J. Sheng and C. Zi, *Struct. Chem.*, **33**, 795 (2022); <https://doi.org/10.1007/s11224-022-01895-2>
50. V. Deepha, R. Praveena and K. Sadasivam, *J. Mol. Struct.*, **1082**, 131 (2014); <https://doi.org/10.1016/j.molstruc.2014.10.078>
51. R.P. Gangadharan and S.S. Krishnan, *Acta Phys. Pol. A*, **125**, 18 (2014); <https://doi.org/10.12693/APhysPolA.125.18>